Kar2p Availability Defines Distinct Forms of Endoplasmic Reticulum Stress in Living Cells

Patrick Lajoie[*], Robyn D. Moir[†], Ian M. Willis[†‡], and Erik L. Snapp[*§]

[*]Department Anatomy and Structural Biology, [†]Department of Biochemistry, and [‡]Department of Systems and Computational Biology
Albert Einstein College of Medicine of Yeshiva University
Bronx, NY, USA 10461

[§]Corresponding author:
Erik Lee Snapp, PhD
Department of Anatomy and Structural Biology
Albert Einstein College of Medicine
1300 Morris Park Ave.
Bronx, NY 10461

Email: erik-lee.snapp@einstein.yu.edu
Phone: 718-430-2967

Running Head: Detecting Unfolded Secretory Protein Levels

Abbreviations used:
CHX: cycloheximide
D: effective Diffusion coefficient
DTT: Dithiothreitol
ER: Endoplasmic Reticulum
ERAD: Endoplasmic Reticulum Associated Degradation
FLIP: Fluorescence Loss In Photobleaching
FRAP: Fluorescence Recovery After Photobleaching
GFP: Green Fluorescent Protein
MFI: Median Fluorescence Intensity
QC: Quality Control
ROI: Region of Interest
SFGFP: Superfolder GFP
Tm: Tunicamycin
UPR: Unfolded Protein Response

ABSTRACT

Accumulation of misfolded secretory proteins in the endoplasmic reticulum (ER) activates the Unfolded Protein Response (UPR) stress pathway. To enhance secretory protein folding and promote adaptation to stress, the UPR upregulates ER chaperone levels, including BiP. Here, we describe chromosomal tagging of *KAR2,* the yeast homolog of BiP, with superfolder GFP (sfGFP) to create a multifunctional endogenous reporter of the ER folding environment. Changes in Kar2p-sfGFP fluorescence levels directly correlate with UPR activity and represent a robust reporter for high throughput analysis. A novel second feature of this reporter is that photobleaching microscopy (FRAP) of Kar2p-sfGFP mobility reports on the levels of unfolded secretory proteins in individual cells, independent of UPR status. Kar2p-sfGFP mobility decreases upon treatment with tunicamycin or DTT, consistent with increased levels of unfolded proteins and the incorporation of Kar2p-sfGFP into slower diffusing complexes. During adaptation, we observe a significant lag between downregulation of the UPR and resolution of the unfolded protein burden. Finally, we find Kar2p-sfGFP mobility significantly increases upon inositol withdrawal, which also activates the UPR, apparently independent of unfolded protein levels. Thus, Kar2p mobility represents a powerful new tool capable of distinguishing between the different mechanisms leading to UPR activation in living cells.

INTRODUCTION

Proper secretory protein folding in the endoplasmic reticulum (ER) is essential for the maintenance of homeostasis and cell viability. The eukaryotic cell has evolved machinery and signaling pathways to enhance secretory protein folding and stability (Brodsky and Skach, 2011). In the ER, various chaperones directly assist folding of nascent peptides as they enter the ER lumen (Ma and Hendershot, 2004). The quality control (QC) machinery remodels the newly synthesized protein via multiple posttranslational modifications, including formation of disulfide bonds (Feige and Hendershot, 2011) and N-linked glycosylation (Hulsmeier *et al.*, 2011). Failure to correctly complete these tasks can result in a misfolded protein. If accumulation of misfolded protein exceeds the capacity of the ER QC machinery, the cell enters a state of ER stress. To cope with accumulation of misfolded proteins, the cell can activate an adaptive program termed the Unfolded Protein Response (UPR) (Ron and Walter, 2007). UPR sensors monitor the ER lumen for increased levels of misfolded proteins and then initiate the UPR (Kimata and Kohno, 2011). In yeast, the sole UPR sensor is the endoribonuclease Ire1p (Mori, 2009). During UPR activation, Kar2p releases from the luminal domain of Ire1p enabling Ire1p dimerization (Oikawa *et al.*, 2005). The Ire1p dimers undergo transautophosphorylation, assemble into clusters (Kimata *et al.*, 2007; Aragon *et al.*, 2009), and activate the site-specific RNase domain of the protein (Sidrauski and Walter, 1997). Ire1p cleaves *HAC1* mRNA to remove a 252 nucleotide intron to generate the spliced functional form of the mRNA (Cox and Walter, 1996; Ruegsegger *et al.*, 2001). The resulting translated Hac1p transcription factor upregulates numerous cell functions including transcription of genes encoding ER QC machinery including chaperones, such as Kar2p (Harding *et al.*, 1999)

and ER associated protein degradation (ERAD) components (Yoshida *et al.*, 2003). Hac1p also stimulates ER membrane expansion (Bernales *et al.*, 2006; Schuck *et al.*, 2009). These changes increase the folding capacity of the ER and can enable a return to homeostasis. Therefore, UPR signaling is critical during ER stress (Chawla *et al.*, 2011; Rubio *et al.*, 2011) and failure to generate an adaptive UPR can result in cell death (Hetz *et al.*, 2006; Tabas and Ron, 2011).

Cells are described as experiencing ER stress if they exhibit activation of the UPR components. Binding of accumulated misfolded proteins by Ire1p has been shown to directly activate the UPR in yeast (Gardner and Walter, 2011; Promlek *et al.*, 2011). The classical markers of ER stress include Ire1p activation, *HAC1* splicing, and increased Kar2p levels (Kimata and Kohno, 2011). In contrast to these readily measurable parameters, it has proven difficult to quantitate the global levels of unfolded protein accumulating in the ER lumen during the UPR. Moreover, most reporters rely on aspects of UPR sensor function and therefore cannot measure ER stress in cells with compromised UPR signaling. Our lab recently developed a method to measure the unfolded protein burden in living cells that exploits the ability of the chaperone BiP (the mammalian Kar2p homologue) to recognize and directly bind unfolded proteins (Lai *et al.*, 2010; Lajoie and Snapp, 2011). Using the technique of fluorescence recovery after photobleaching (FRAP), we demonstrated that GFP-tagged BiP diffusional mobility correlates with unfolded protein accumulation independent of the status of the UPR. In mammalian cells, this assay is complicated by the presence of endogenous BiP, which probably masks the full extent of BiP occupancy. Here, we have circumvented this limitation by chromosomal tagging of *KAR2* in budding yeast with the super folder variant of GFP (Janke *et al.*, 2004; Pedelacq *et al.*, 2006). This new endogenous reporter allowed us to 1) confirm the appropriate localization and function of Kar2p-sfGFP, 2) directly quantify unfolded protein accumulation in cells independent of UPR activation, and 3) investigate the effects of various forms of ER stress on the unfolded protein burden in living cells independent of and relative to UPR activation.

RESULTS

Generation of Endogenous Kar2p-sfGFP

To generate an endogenous fluorescent Kar2p variant, we exploited the high efficiency of homologous recombination in yeast and the ability to perform chromosomal tagging of endogenous genes with fluorescent proteins (Huh *et al.*, 2003). Two important modifications to previous efforts involving GFP tagging were incorporated. First, our lab recently established that the improved folding capacity of super folder GFP (sfGFP) prevents significant misfolding of GFP via inappropriate disulfide bonds and minimizes the formation of non-fluorescent species in oxidizing environments, including the ER (Aronson *et al.*, 2011). Therefore, we used sfGFP for our tagging efforts. Second, it was previously reported that yeast cells carrying Kar2p-GFP were viable, but the cellular localization of the fusion protein was ambiguous (Huh *et al.*, 2003). This result could be partially explained by disruption of the ER retrieval motif, -HDEL, on the resulting fusion protein (Munro and Pelham, 1987; Snapp, 2009). Therefore, we added an HDEL motif to the C-terminus of the sfGFP to restore HDEL mediated slowing of the loss of

Kar2p from the ER (Figure 1A). The sfGFP-HDEL construct, along with a *HIS3* selectable marker, was integrated at the *KAR2* locus. Successful tagging of the gene and production of the Kar2p-sfGFP fusion protein was confirmed by immunoblot for both Kar2p and sfGFP (Figure 1C). Imaging of live cells expressing Kar2p-sfGFP revealed a typical pattern of peripheral and nuclear ER fluorescence expected for an ER localized protein (Figure 1B).

Next, we established the functionality of the Kar2p-sfGFP protein. *KAR2* is essential for cell viability (Normington *et al.*, 1989). *KAR2* conditional mutants are unable to rescue cells from low levels of ER stressors such as tunicamycin (Tm), an inhibitor of N-glycosylation (Rose *et al.*, 1989; Kimata *et al.*, 2003) or elevated temperature, i.e. 37°C. The Kar2p-sfGFP strain grew well on synthetic media and grew only slightly less well on Tm-containing media relative to the wildtype strain (Figure 1D). For comparison, *ire1Δ* cells, which cannot induce the UPR, were unable to survive on Tm. Moreover, when cultured at 37°C Kar2p-sfGFP cells grew robustly (Figure 1D). This contrasts with temperature sensitive *KAR2* mutants, which grow robustly at the permissive temperature of 22°C and grow poorly at higher temperatures (Polaina and Conde, 1982; Kimata *et al.*, 2007).

To further characterize the Kar2p-sfGFP fusion protein, we investigated whether the sfGFP fusion on Kar2p affected UPR regulation. A plasmid containing the fluorescent UPR reporter, UPR-mCherry (Merksamer *et al.*, 2008), was introduced into wildtype and Kar2p-sfGFP yeast strains. The reporter mCherry expression is driven by a minimal CYC1 promoter and four tandem UPR elements and thus, should be expressed only during ER stress. The fluorescence intensity of UPR-mCherry was recorded by flow cytometry (Figure 1E) in untreated and DTT-treated (which prevents the formation of disulfide bonds in nascent secretory proteins) strains. In addition, the splicing of *HAC1* mRNA in response to DTT-mediated UPR activation was assessed directly by northern analysis (Figure 1F). Together, these results established two important features of the chromosomally tagged Kar2p-sfGFP strain. First, the GFP fusion does not constitutively activate the UPR at steady state. Second, Kar2p-sfGFP cells can induce a robust UPR in response to unfolded protein stress. Note that efficient release of Kar2p from Ire1p is required for UPR activation and Kar2p binding and release of substrates correlates with regulated UPR activation (Kimata *et al.*, 2003). However, Ire1p mutants defective in Kar2p binding do not exhibit constitutive UPR, arguing that Kar2p buffers against unfolded protein levels and modulates the stress response rather than directly regulating Ire1p activation (Kimata *et al.*, 2004; Oikawa *et al.*, 2009; Pincus *et al.*, 2010).

Next, we asked whether we could monitor Kar2p-sfGFP levels in living cells during ER stress as a proxy for UPR activation. *KAR2* is a classic UPR target gene and its expression increases following treatment with ER stressors including DTT and Tm (Travers *et al.*, 2000). We treated Kar2p-sfGFP cells with either ER stressor and quantified the fluorescence levels by microscopy and flow cytometry. The Kar2p-sfGFP signal increased nearly 10-fold after a 4 h treatment either Tm or DTT (Figure 2A and B). The increase in Kar2p-sfGFP signal was dependent on stress activation of the UPR, since no change in Kar2p-sfGFP fluorescence intensity was observed in an *ire1Δ* strain (Figure 2C). Moreover, the change in Kar2p-sfGFP fluorescence signal was specific since the fluorescence intensity of the inert reporter ER-sfGFP-HDEL did not change in response to DTT treatment (Figure 2D). Finally, the comparable accumulation of wildtype and

Kar2p-sfGFP proteins in response to ER stress indicates that the addition of the sfGFP tag preserves the UPR regulation of target genes, including Kar2p (Figure 2E). These results demonstrate that the Kar2p-sfGFP fusion protein robustly reports on UPR activation by both standard microscopy and by high throughput methods, including flow cytometry.

ER Lumen Unfolded Protein Burden and Kar2p Availability

We previously used fluorescence microscopy techniques to establish in mammalian cells that the decrease of BiP-GFP mobility reflects binding of the chaperone to unfolded protein substrates (Lai *et al.*, 2010; Lajoie and Snapp, 2011). We asked whether Kar2p-sfGFP would function comparably as a reporter of unfolded protein accumulation. First, the mobility of Kar2p-sfGFP was assessed using Fluorescence Loss in Photobleaching (FLIP) (Ellenberg *et al.*, 1997). For this technique, a discrete region of interest (ROI) within the cells is repeatedly photobleached while images are acquired. If the protein is mobile within a continuous compartment, the total fluorescence within this compartment will eventually be depleted by FLIP. In unstressed cells, Kar2p-sfGFP is mobile throughout the ER (Figure 3A, top panels), similar to our previous results with BiP-GFP in mammalian cells (Lai *et al.*, 2010). Total cellular fluorescence was homogenously depleted within a short time window (Figure 3A), indicating that Kar2p-sfGFP is not immobilized or enriched in ER subdomains. Treatment with ER stressors, Tm or DTT, significantly decreased the mobility of Kar2p-sfGFP as demonstrated by the longer time interval required to deplete 50% of the GFP fluorescence (control: 125s, +Tm: 230 s, + DTT 315 s) (Figure 3A, lower panels and Figure 3B). Importantly, the GFP fluorescence was ultimately homogenously depleted in the Kar2p-sfGFP strain, excluding the possibility that Kar2p-sfGFP becomes trapped or incorporated into a chaperone matrix following acute ER stress (Pfeffer and Rothman, 1987).

A potential caveat for interpreting these measurements is that soluble protein mobility is impacted both by the size of the molecule and the viscosity of its environment (Einstein, 1905). ER luminal viscosity in living cells can be assessed with inert fluorescent protein probes (Snapp *et al.*, 2006; Lai *et al.*, 2010), such as ER targeted sfGFP, which has no known interacting partners. In this case, treatment with Tm or DTT modestly reduces mobility of ER-sfGFP-HDEL (Figure 3C and D). The time intervals to deplete 50% of the GFP fluorescent were 20 s for the control and 30 s for both Tm and DTT treated cells. Thus, treatment with ER stressors does not induce gross changes in the ER environment that disrupt ER continuity or immobilize pools of ER luminal proteins. Importantly, the FLIP loss of fluorescence of ER-sfGFP-HDEL in treated cells was significantly more rapid than for the much larger Kar2p-sfGFP. These data are consistent with our previous finding in mammalian cells, where slower BiP-GFP mobility correlated with binding of the chaperone to substrate.

To further characterize Kar2p substrate binding in yeast, we quantified the mobility of Kar2p-sfGFP using Fluorescence Recovery after Photobleaching (FRAP). During FRAP experiments, changes in the mobility or molecular availability of the fluorescently tagged protein are reflected by the effective diffusion coefficient (*D*). Changes in *D* report on changes in the environment viscosity, size of the molecule or its incorporation into or release from molecular complexes (Snapp *et al.*, 2003b). In

mammalian cells, the mobility of BiP-GFP was shown to increase after substrate depletion by translational inhibition and with loss of function in the BiP-GFP substrate-binding domain (Lai *et al.*, 2010). FRAP analysis of Kar2p mobility in yeast ER was similarly responsive to substrate depletion (Figure 4A). A significant increase in *D* was observed following treatment of yeast with the translational inhibitor cycloheximide (CHX) for 30 min (Figure 4B) consistent with depletion of substrate and increased Kar2p-sfGFP availability. We hypothesized that if Kar2p-sfGFP mobility reflects binding of Kar2p to misfolded proteins, then *D* should decrease as the unfolded protein burden increases. To test this hypothesis, cells were treated with Tm for 2 h and analyzed by FRAP. Indeed, there was a significant decrease in *D* following Tm treatment (Figure 4B). Interestingly, when cells were treated with Tm for 90 min and CHX was added for the last 30 min of treatment, we observed a significant increase in *D* (Figure 4B). The latter result indicates that while Tm prevents glycosylation of nascent proteins, the inhibition of protein synthesis can decrease the Tm-induced misfolded protein burden and result in increased Kar2p-sfGFP mobility in stressed cells. These data support a role for Kar2p substrate levels as a major contributing factor in affecting Kar2p-sfGFP mobility.

Next, the reversibility of Kar2p-sfGFP substrate binding was assessed using DTT treatment, which induces reversible protein unfolding (Braakman *et al.*, 1992; Lai *et al.*, 2010). Washout of DTT permits unfolded secretory proteins to release from ER chaperones and refold (Simons *et al.*, 1995) and is accompanied by a gradual loss of UPR signaling as reported by *HAC1* mRNA splicing and Ire1p clustering (Pincus *et al.*, 2010). The mobility of Kar2p-sfGFP decreased after DTT treatment to a comparable extent as detected with Tm treatment (Figure 4C). Consistent with the reversibility of the DTT induced protein misfolding, Kar2p-sfGFP mobility was restored after washout of DTT, approaching the mobility level detected in untreated cells.

The increase in ER chaperone and other UPR targeted proteins in response to ER stress (e.g. the 10-fold increase in Kar2p protein levels, Figure 2C and D) has the potential to alter ER lumen crowdedness and affect ER-sfGFP-HDEL mobility. Although the FLIP results (Figure 3C and D) did not indicate a gross change in the mobility of the inert ER-sfGFP-HDEL reporter in response to ER stress, we quantified the effect of ER stress on ER environment viscosity using FRAP using the ER-sfGFP strain. Treatment with either DTT or Tm (Figure 4D) decreased ER-sfGFP-HDEL mobility by ~25%. A comparable decrease was detected in *ire1*Δ cells (Figure S3), indicating that the effect is independent of the canonical UPR. The small diameter of ER tubules is conserved from yeast to mammalian cells (40-70 nm) (Voeltz *et al.*, 2002) and may limit the diffusional mobility of luminal proteins once unfolded proteins accumulate in response to Tm or DTT treatment. Indeed, we observed no changes in ER-sfGFP-HDEL mobility in most mammalian cell lines during ER stressor treatment (Lai *et al.*, 2010; Lajoie and Snapp, 2011). Nonetheless, the mobility decrease observed for Kar2p-sfGFP (>70%) is significantly greater than the decrease in *D* of the inert reporter (~35%). Moreover, Kar2p mobility is sensitive to CHX (Figure 4B) while ER-sfGFP-HDEL mobility is not. Together these data argue that changes in Kar2p-sfGFP mobility predominantly reflect its binding to substrate.

One challenge to dissecting the various cellular events that impact UPR activation has been the ability to robustly quantify changes in unfolded protein accumulation in the ER lumen at any given time. Our studies in mammalian cells, using the BiP-GFP

mobility assay, demonstrated that changes in unfolded protein burden can be detected independent of the UPR pathway (Lai *et al.*, 2010). These analyses were however limited to cells with functional UPR machinery. The Kar2p-sfGFP mobility assay in *S. cerevisiae* allowed us to assess changes in the ER unfolded protein burden in the absence of a functional UPR (*ire1Δ* cells). In unstressed *ire1Δ* cells, Kar2p-sfGFP mobility was significantly lower than that of wildtype cells (Figure 4E). There was no difference in ER-sfGFP-HDEL mobility (Figure 4F). The viability of *ire1Δ* cells and their lack of gross growth defects under non-stressful conditions (Fig 1D), suggests that the decrease in Kar2p-sfGFP mobility in the untreated *ire1Δ* cells reflects higher, but non-lethal steady state levels of unfolded protein. Treatment of *ire1Δ* cells with 0.025 μg/ml Tm further decreased Kar2p-sfGFP mobility (Figure 4E) consistent with their hypersensitivity to ER stressors (Figure 1D). Kar2p-sfGFP mobilities were indistinguishable between wildtype and mutant cells treated with a high dose of Tm (Figure 4E). Importantly, the Kar2p-sfGFP mobility assay enabled quantitation of the misfolded protein burden in the ER of cells with compromised UPR signaling. To date, the only measure of ER stress independent of UPR signaling has been the quantitation of ER redox potential using a GFP reporter (Merksamer *et al.*, 2008). The Kar2p-sfGFP mobility assay not only allows detection of unfolded protein levels under various conditions, but also reports on differences in unfolded protein levels in unstressed cells of various genetic backgrounds (Merksamer *et al.*, 2008; Pincus *et al.*, 2010).

Just as it is important for cells to cope with an unfolded secretory protein stress, the ability of cells to resolve the UPR, itself, is critical for survival. Yeast demonstrably overcome chemical-mediated unfolded secretory protein stresses and attenuate the UPR (Pincus *et al.*, 2010; Chawla *et al.*, 2011; Rubio *et al.*, 2011). However, yeast expressing Ire1p mutants unable to attenuate the UPR are hypersensitive to tunicamycin and DTT stressors (Chawla *et al.*, 2011; Rubio *et al.*, 2011). Implicit to these problems is whether there is a correlation between resolution of the unfolded protein stress and attenuation of the UPR. That is, is the UPR attenuated at the time that the unfolded protein burden has been resolved? Therefore, we investigated Kar2p availability before and after UPR attenuation.

To assess UPR status in live cells, we used a fluorescent reporter (SR-GFP), which directly reports on the endonuclease activity of Ire1p (Pincus *et al.*, 2010). The increasing fluorescent signal in stressed cells, expressing the reporter, was measured by flow cytometry (Figure 5A). Cells were treated with 1 μg/ml Tm, a dose sufficient to activate the UPR. Wild-type cells can attenuate the UPR from this Tm dose ~4 h later and continue growing (Figure 1D), consistent with adaptation to this level of unfolded protein stress (Chawla et al., 2011). After 4 h, the median GFP fluorescence reached an asymptote (Figure 5A). The plateau in intensity indicates no additional stress has been detected and signaled (Pincus *et al.*, 2010). The GFP signal persists for several hours as a consequence of the long half-life of GFP. Thus, a plateau reports on attenuation of Ire1p endonuclease activity and restoration of the folding capacity of the ER. FRAP at 4 h of Tm treatment revealed significantly reduced Kar2p-sfGFP mobility. After this time, no significant increase in UPR reporter fluorescence was observed. In contrast, it was only after 16 h of Tm treatment, Kar2p-sfGFP mobility returned to *D* values comparable with untreated cells (Figure 5B). The restored mobility is unlikely to reflect the loss of Tm activity, since the media of Tm-treated cells can be used to induce UPR in naive cells

(Chawla *et al.*, 2011). Therefore, we conclude that the ER folding capacity was restored. UPR-mediated increases in levels of chaperones, ERAD and secretion components, the ALG7 gene product (the target of Tm), and upregulation of proteasomal activity probably all account for the decrease in ER misfolded protein in adapted cells.

These results lead to the somewhat surprising conclusion that UPR inactivation occurs even while a substantial unfolded protein burden remains. We hypothesize that UPR attenuation likely occurs when the stressed ER achieves a small (below our limit of detection) increase in the available pool of Kar2p and potentially other quality control machinery components. Simultaneously or in parallel, Ire1p regulatory attenuators, such as the phosphatase Ptc2p (Welihinda *et al.*, 1998)may achieve a sufficient level of activity to turn off the UPR. While these matters remain speculative, the results suggest that tools capable of measuring the instantaneous status of UPR activity will be needed to understand the temporal and mechanistic aspects of UPR attenuation.

Kar2p Mobility Distinguishes Various Forms of UPR

Finally, we investigated the ability of our FRAP assay to distinguish between different types of UPR activation. The UPR is generally considered to be dependent on increased levels of unfolded proteins (Credle *et al.*, 2005; Kimata *et al.*, 2007; Gardner and Walter, 2011; Kimata and Kohno, 2011). Recently, however, it was shown that UPR activation by either inositol depletion or deletion of lipid biosynthetic genes does not require the luminal unfolded peptide-binding portion of Ire1p (Promlek *et al.*, 2011). Thus, lipid imbalance can lead to UPR activation independently of the accumulation of unfolded proteins; distinct from of the response to the classic ER stressors Tm and DTT. We asked how the Kar2p-sfGFP and UPR-mCherry reporters respond to perturbation of lipid metabolism. In the absence of inositol, the phosphatidic acid levels on the ER are high and genes involved in inositol biosynthesis and phospholipid metabolism are actively transcribed (Carman and Henry, 2007). Inositol depletion increased expression of both Kar2p-sfGFP and UPR-mCherry reporters, indicating UPR activation (Figs. 6A and B). Next, the effect of inositol depletion on Kar2p-sfGFP mobility was examined by FRAP. Despite strong evidence of UPR activation, inositol depletion did *not* decrease Kar2p-sfGFP mobility, unlike the effect of Tm treatment (Figure 6B). On the contrary, the Kar2p-sfGFP mobility increased, paralleling the increase in Kar2p-sfGFP intensity (Figure 6B). The increased mobility may reflect a higher Kar2p/substrate ratio that leads to an increase in unbound Kar2p. Inositol depletion did not significantly change the mobility of the inert ER-sfGFP-HDEL, indicating that the increase in Kar2p mobility was independent of ER viscosity (Figure 6C). Therefore, various stresses appear to activate Ire1p and elicit the UPR by distinct mechanisms. Kar2p-sfGFP mobility represents a novel non-invasive assay to distinguish between these different forms of UPR in intact cells.

DISCUSSION

The ability to evaluate unfolded protein accumulation in the ER, independent of the UPR, should now enable novel analyses of how cells sense and cope with different environmental stresses. Our Kar2p-sfGFP reporter has the advantage of reporting

simultaneously on both the activation of UPR and changes in the unfolded protein burden. In this study, Kar2p-sfGFP has allowed us to distinguish between two distinct forms of stress capable of activating the UPR (Figure 7). This study, and the work of other groups, now suggest that lipid imbalance can lead to activation of the yeast UPR (Pineau *et al.*, 2009; Deguil *et al.*, 2011; Promlek *et al.*, 2011). However, the mechanisms by which changes in ER membrane lipid composition lead to Ire1p activation remain unclear. A recent study described a mutant Ire1p (ΔIII mutant) unable to bind misfolded peptides and was therefore insensitive to DTT or tunicamycin treatment, but could still be activated upon inositol depletion (Promlek *et al.*, 2011). Our study and the Promlek et al. study appear to conflict with another study reporting that activation of the UPR by accumulation of fatty acids occurs via accumulation of misfolded protein. The argument was supported by the ability to block fatty acid-induced UPR with the chemical chaperone 4-phenyl butyrate (Pineau *et al.*, 2009). We argue that our direct measure of the unfolded protein burden combined with the data from the Promlek et al. study strongly support the existence of a novel activation mechanism for Ire1p, at least for some stresses. Thus, inositol depletion-stimulated Ire1p activation represents at least one alternative pathway that differs from the classical Ire1p activation pathway involving direct binding of the stress sensor to misfolded peptides (Kimata *et al.*, 2007; Gardner and Walter, 2011). An important implication of this study is that either Ire1p or a hypothetical binding partner contains at least one additional regulatory site for activation.

Understanding how changes in inositol and other lipids regulate Ire1p will be important for understanding the fundamental biology of the UPR and may have implications for drug development. Therapeutic targets for positive and negative regulation of UPR sensors could be present at this regulatory site. Upregulation of Kar2p-sfGFP fluorescence provides a non-invasive method to monitor UPR activation in living cells and is suitable for high throughput screens. Our Kar2p-sfGFP reporter should enable novel interrogation of cells to characterize modulators of the ER folding capacity relative to UPR activation under homeostatic, stressed, and adapted states in various genetic backgrounds.

MATERIALS AND METHODS

Drugs

Stock solutions of DTT (Fisher Scientific, Pittsburgh, PA) (1M in water), Tm (Calbiochem, La Jolla, CA) (5 mg/ml in DMSO) and CHX (Sigma-Aldrich, St. Louis, MO) (5 mg/ml in water) were prepared and used at the concentrations and times indicated

Strains and Cell Growth

See Table I for all yeast strains in this study. SfGFP was chromosomally integrated into *KAR2* in wild-type and mutant strains using standard PCR methodology (Janke *et al.*, 2004). All yeast strains were grown in synthetic complete media (SC) supplemented with 400 μM inositol and appropriate amino acids at 30°C. Yeast strains were grown overnight to early log phase (OD_{600nm} ~0.5) for analysis. For DTT washout experiments, cells were incubated with 5mM DTT for 30 min, then pelleted and resuspended in fresh media and incubated for 4 h before processing for FRAP. For inositol depletion

experiments, cells were pelleted, washed twice with inositol-free media and incubated for various amounts of time in absence of inositol.

Plasmid construction

UPR-mCherry (Merksamer *et al.*, 2008) was obtained from Addgene (Cambridge, MA). SR-GFP was obtained from Dr. Peter Walter (University of California at San Francisco). The KDEL retrieval motif inserted at the C-terminus of the sfGFP–N1 plasmid (Pedelacq *et al.*, 2006; Lai *et al.*, 2010) was modified to contain the yeast HDEL motif using the following primers:

F-GGACGAGCTGTACAAGGATGAATTGTAAGCG
R-CGCTTACAATTCATCGTGGTACAGCTCGTCC

An amplifiable cassette of sfGFP-HDEL was generated in the yeast PCR plasmid pYM28 (Janke *et al.*, 2004) by substituting sfGFP-HDEL for EGFP at SalI/BamH1 sites. The following primers were used to amplify the sfGFP-HDEL cassette from sfGFP–N1:

F- GATCGTCGACATGGTGAGCAAGGGC
R –GATCGGATCCTTACAATTCATCGTG

The sfGFP-HDEL module can be amplified using the original S2 and S3 primers and the original *HIS3MX6* selection marker.

ER-sfGFP-HDEL was made by inserting the first 135 base pairs of the Kar2p coding sequence (Rossanese *et al.*, 2001) fused into the BglII/AgeI sites of sfGFP-HDEL using the following primers:

F- GATCAGATCTCTAAAAATGTTTTTCAACAGAC
R-GATCACCGGTCCATCATCGGCACCTCTAAC.

The ER-sfGFP-HDEL fragment was subsequently amplified using the following primers:

F- GCAAATGGGCGGTAGGCG
R-GATCGGATCCTTACAATTCATCGTG.

The resulting fragment was digested with BglII and BamHI and cloned into the BamHI site of pRS415-GPD (a generous gift from Dr. Elizabeth Miller, Columbia University, New York, NY).

Fluorescence microscopy, FRAP, and FLIP

After incubation with various stressors, log phase cells were placed in 8 well Labtek chambers (Thermo Fisher Inc.) and allowed to settle for 5 minutes before imaging. Cells were imaged an Axiovert 200 widefield fluorescence microscope (Carl Zeiss Microimaging Inc.) with a 63X oil NA 1.4 objective, a 450–490 excitation/500–550 emission bandpass filter and a Retiga 2000R camera. Image analysis was performed with ImageJ (National Institutes of Health; Bethesda, MD).

For FRAP and FLIP, live cells were imaged on a Duoscan confocal microscope system (Carl Zeiss Microimaging, Jena, Germany) with a 63X NA1.4 oil objective and a

489 nm 100 mW diode laser with a 500–550 nm bandpass filter for GFP. FRAP and FLIP experiments were performed by photobleaching a region of interest at full laser power of the 489 nm line and monitoring fluorescence loss or recovery over time. No photobleaching of the adjacent cells during the processes was observed. *D* measurements were calculated using an inhomogeneous diffusion simulation, as described previously (Siggia *et al.*, 2000; Snapp *et al.*, 2003a).

Immunoblots

Early log phase Kar2p and Kar2p-sfGFP strains, untreated or treated with Tm, were pelleted and total protein extracted by alkaline lysis (Kushnirov, 2000). Lysates were separated on 7.5% SDS-PAGE tricine gels, transferred to nitrocellulose membranes and detected with anti-GFP (from Dr. Ramanujan Hegde, MRC Laboratory of Molecular Biology, Cambridge, UK), anti-Kar2p (from Dr. Peter Walter, UCSF, San Francisco, CA), anti-Rpl5p (from Dr. Jonathan Warner, Albert Einstein College of Medicine, Bronx, NY) or HRP-labeled anti-rabbit (Jackson Immunoresearch Laboratories, West Grove, PA).

Northern Blot

RNA extraction, northern analysis and quantitation are as previously described (Li *et al.*, 2000). Early log phase Kar2p and Kar2p-sfGFP yeast strains, untreated or treated with DTT, were pelleted on ice to preserve RNA intermediates and quickly frozen. Total RNA was extracted by the glass-bead hot-phenol method (O'Connor and Peebles, 1991). RNA was analyzed on 5% agarose gels containing 6% formaldehyde. After transfer to Nytran plus membranes, blots were probed with [^{32}P]-labeled oligonucleotides, washed, and imaged with a storm 820 phosphorimager (GE Healthcare, Pittsburgh, PA).

Flow cytometry

Early log phase cells expressing the various plasmids were treated with ER stressors as described in the text. Cells were pelleted, resuspended in PBS containing 2% glucose and analyzed by flow cytometry using an BD LSRII equipped with a 488 nm laser with a 525/50 bandpass filter for sfGFP and a 561 nm laser with a 610/20 bandpass filter for mCherry and FACSDIVA software to compile .fcs files. The files were analyzed using FloJo. No gates were applied. Median fluorescence intensities were calculated for each channel and plotted in Prism (5.0c) (GraphPad Software Inc., La Jolla, CA). Errors bars represent the standard deviation of the median of three biological replicates.

ACKNOWLEDGMENTS

We thank Dr. Ramanujan Hegde for the anti-GFP antibody, Dr. Peter Walter for the anti-Kar2p antibody and the SR-GFP vector, Dr. Jonathan Warner for the anti-Rpl5p antibody, and Dr. Elizabeth Miller for the p415-GPD vector. This study was supported by National Institutes of Health grants, NIGMS RO1GM086530-01 to ELS and RO1GM085177 to IMW and a National Cancer Institute center support grant P30CA013330 to the Einstein Flow Cytometry Core facility.

REFERENCES

Aragon, T., van Anken, E., Pincus, D., Serafimova, I.M., Korennykh, A.V., Rubio, C.A., and Walter, P. (2009). Messenger RNA targeting to endoplasmic reticulum stress signalling sites. Nature *457*, 736-740.

Aronson, D.E., Costantini, L.M., and Snapp, E.L. (2011). Superfolder GFP is fluorescent in oxidizing environments when targeted via the Sec translocon. Traffic *12*, 543-548.

Bernales, S., McDonald, K.L., and Walter, P. (2006). Autophagy counterbalances endoplasmic reticulum expansion during the unfolded protein response. PLoS Biol *4*, e423.

Braakman, I., Helenius, J., and Helenius, A. (1992). Manipulating disulfide bond formation and protein folding in the endoplasmic reticulum. EMBO J *11*, 1717-1722.

Brodsky, J.L., and Skach, W.R. (2011). Protein folding and quality control in the endoplasmic reticulum: Recent lessons from yeast and mammalian cell systems. Curr Opin Cell Biol *23*, 464-475.

Carman, G.M., and Henry, S.A. (2007). Phosphatidic acid plays a central role in the transcriptional regulation of glycerophospholipid synthesis in Saccharomyces cerevisiae. J Biol Chem *282*, 37293-37297.

Chawla, A., Chakrabarti, S., Ghosh, G., and Niwa, M. (2011). Attenuation of yeast UPR is essential for survival and is mediated by IRE1 kinase. J Cell Biol *193*, 41-50.

Cox, J.S., and Walter, P. (1996). A novel mechanism for regulating activity of a transcription factor that controls the unfolded protein response. Cell *87*, 391-404.

Credle, J.J., Finer-Moore, J.S., Papa, F.R., Stroud, R.M., and Walter, P. (2005). On the mechanism of sensing unfolded protein in the endoplasmic reticulum. Proc Natl Acad Sci U S A *102*, 18773-18784.

Deguil, J., Pineau, L., Rowland Snyder, E.C., Dupont, S., Beney, L., Gil, A., Frapper, G., and Ferreira, T. (2011). Modulation of lipid-induced ER stress by fatty acid shape. Traffic *12*, 349-362.

Einstein, A. (1905). Über die von der molekularkinetischen Theorie der Wärme

geforderte Bewegung von in ruhenden Flüssigkeiten suspendierten Teilchen. Ann Phys *17*, 549-560.

Ellenberg, J., Siggia, E.D., Moreira, J.E., Smith, C.L., Presley, J.F., Worman, H.J., and Lippincott-Schwartz, J. (1997). Nuclear membrane dynamics and reassembly in living cells: targeting of an inner nuclear membrane protein in interphase and mitosis. J Cell Biol *138*, 1193-1206.

Feige, M.J., and Hendershot, L.M. (2011). Disulfide bonds in ER protein folding and homeostasis. Curr Opin Cell Biol *23*, 167-175.

Gardner, B.M., and Walter, P. (2011). Unfolded Proteins Are Ire1-Activating Ligands that Directly Induce the Unfolded Protein Response. Science. *333*, 1891-4

Harding, H.P., Zhang, Y., and Ron, D. (1999). Protein translation and folding are coupled by an endoplasmic-reticulum-resident kinase. Nature *397*, 271-274.

Hetz, C., Bernasconi, P., Fisher, J., Lee, A.H., Bassik, M.C., Antonsson, B., Brandt, G.S., Iwakoshi, N.N., Schinzel, A., Glimcher, L.H., and Korsmeyer, S.J. (2006). Proapoptotic BAX and BAK modulate the unfolded protein response by a direct interaction with IRE1alpha. Science *312*, 572-576.

Huh, W.K., Falvo, J.V., Gerke, L.C., Carroll, A.S., Howson, R.W., Weissman, J.S., and O'Shea, E.K. (2003). Global analysis of protein localization in budding yeast. Nature *425*, 686-691.

Hulsmeier, A.J., Welti, M., and Hennet, T. (2011). Glycoprotein maturation and the UPR. Methods Enzymol *491*, 163-182.

Janke, C., Magiera, M.M., Rathfelder, N., Taxis, C., Reber, S., Maekawa, H., Moreno-Borchart, A., Doenges, G., Schwob, E., Schiebel, E., and Knop, M. (2004). A versatile toolbox for PCR-based tagging of yeast genes: new fluorescent proteins, more markers and promoter substitution cassettes. Yeast *21*, 947-962.

Kimata, Y., Ishiwata-Kimata, Y., Ito, T., Hirata, A., Suzuki, T., Oikawa, D., Takeuchi, M., and Kohno, K. (2007). Two regulatory steps of ER-stress sensor Ire1 involving its cluster formation and interaction with unfolded proteins. J Cell Biol *179*, 75-86.

Kimata, Y., Kimata, Y.I., Shimizu, Y., Abe, H., Farcasanu, I.C., Takeuchi, M., Rose, M.D., and Kohno, K. (2003). Genetic evidence for a role of BiP/Kar2 that regulates Ire1 in response to accumulation of unfolded proteins. Mol Biol Cell *14*, 2559-2569.

Kimata, Y., and Kohno, K. (2011). Endoplasmic reticulum stress-sensing mechanisms in yeast and mammalian cells. Curr Opin Cell Biol *23*, 135-142.

Kimata, Y., Oikawa, D., Shimizu, Y., Ishiwata-Kimata, Y., and Kohno, K. (2004). A role for BiP as an adjustor for the endoplasmic reticulum stress-sensing protein Ire1. J Cell Biol *167*, 445-456.

Kushnirov, V.V. (2000). Rapid and reliable protein extraction from yeast. Yeast *16*, 857-860.

Lai, C.W., Aronson, D.E., and Snapp, E.L. (2010). BiP availability distinguishes states of homeostasis and stress in the endoplasmic reticulum of living cells. Mol Biol Cell *21*, 1909-1921.

Lajoie, P., and Snapp, E. (2011). Changes in BiP availability reveal hypersensitivity to acute ER stress in cells expressing mutant huntingtin. J Cell Sci, *124*, 332-43.

Li, Y., Moir, R.D., Sethy-Coraci, I.K., Warner, J.R., and Willis, I.M. (2000). Repression of ribosome and tRNA synthesis in secretion-defective cells is signaled by a novel branch of the cell integrity pathway. Mol Cell Biol *20*, 3843-3851.

Ma, Y., and Hendershot, L.M. (2004). ER chaperone functions during normal and stress conditions. J Chem Neuroanat *28*, 51-65.

Merksamer, P.I., Trusina, A., and Papa, F.R. (2008). Real-time redox measurements during endoplasmic reticulum stress reveal interlinked protein folding functions. Cell *135*, 933-947.

Mori, K. (2009). Signalling pathways in the unfolded protein response: development from yeast to mammals. J Biochem *146*, 743-750.

Munro, S., and Pelham, H.R. (1987). A C-terminal signal prevents secretion of luminal ER proteins. Cell *48*, 899-907.

Normington, K., Kohno, K., Kozutsumi, Y., Gething, M.J., and Sambrook, J. (1989). S. cerevisiae encodes an essential protein homologous in sequence and function to mammalian BiP. Cell *57*, 1223-1236.

O'Connor, J.P., and Peebles, C.L. (1991). In vivo pre-tRNA processing in Saccharomyces cerevisiae. Mol Cell Biol *11*, 425-439.

Oikawa, D., Kimata, Y., Kohno, K., and Iwawaki, T. (2009). Activation of mammalian IRE1alpha upon ER stress depends on dissociation of BiP rather than on direct interaction with unfolded proteins. Exp Cell Res *315*, 2496-2504.

Oikawa, D., Kimata, Y., Takeuchi, M., and Kohno, K. (2005). An essential dimer-forming subregion of the endoplasmic reticulum stress sensor Ire1. Biochem J *391*, 135-142.

Pedelacq, J.D., Cabantous, S., Tran, T., Terwilliger, T.C., and Waldo, G.S. (2006). Engineering and characterization of a superfolder green fluorescent protein. Nat Biotechnol *24*, 79-88.

Pfeffer, S.R., and Rothman, J.E. (1987). Biosynthetic protein transport and sorting by the endoplasmic reticulum and Golgi. Annu Rev Biochem *56*, 829-852.

Pincus, D., Chevalier, M.W., Aragon, T., van Anken, E., Vidal, S.E., El-Samad, H., and Walter, P. (2010). BiP binding to the ER-stress sensor Ire1 tunes the homeostatic behavior of the unfolded protein response. PLoS Biol *8*, e1000415.

Pineau, L., Colas, J., Dupont, S., Beney, L., Fleurat-Lessard, P., Berjeaud, J.M., Berges, T., and Ferreira, T. (2009). Lipid-induced ER stress: synergistic effects of sterols and saturated fatty acids. Traffic *10*, 673-690.

Polaina, J., and Conde, J. (1982). Genes involved in the control of nuclear fusion during the sexual cycle of Saccharomyces cerevisiae. Mol Gen Genet *186*, 253-258.

Promlek, T., Ishiwata-Kimata, Y., Shido, M., Sakuramoto, M., Kohno, K., and Kimata, Y. (2011). Membrane aberrancy and unfolded proteins activate the endoplasmic reticulum stress sensor Ire1 in different ways. Mol Biol Cell *22*, 3520-3532.

Ron, D., and Walter, P. (2007). Signal integration in the endoplasmic reticulum unfolded protein response. Nat Rev Mol Cell Biol *8*, 519-529.

Rose, M.D., Misra, L.M., and Vogel, J.P. (1989). KAR2, a karyogamy gene, is the yeast homolog of the mammalian BiP/GRP78 gene. Cell *57*, 1211-1221.

Rossanese, O.W., Reinke, C.A., Bevis, B.J., Hammond, A.T., Sears, I.B., O'Connor, J., and Glick, B.S. (2001). A role for actin, Cdc1p, and Myo2p in the inheritance of late Golgi elements in Saccharomyces cerevisiae. J Cell Biol *153*, 47-62.

Rubio, C., Pincus, D., Korennykh, A., Schuck, S., El-Samad, H., and Walter, P. (2011). Homeostatic adaptation to endoplasmic reticulum stress depends on Ire1 kinase activity. J Cell Biol *193*, 171-184.

Ruegsegger, U., Leber, J.H., and Walter, P. (2001). Block of HAC1 mRNA translation by long-range base pairing is released by cytoplasmic splicing upon induction of the unfolded protein response. Cell *107*, 103-114.

Schuck, S., Prinz, W.A., Thorn, K.S., Voss, C., and Walter, P. (2009). Membrane expansion alleviates endoplasmic reticulum stress independently of the unfolded protein response. J Cell Biol *187*, 525-536.

Sidrauski, C., and Walter, P. (1997). The transmembrane kinase Ire1p is a site-specific endonuclease that initiates mRNA splicing in the unfolded protein response. Cell *90*, 1031-1039.

Siggia, E.D., Lippincott-Schwartz, J., and Bekiranov, S. (2000). Diffusion in inhomogeneous media: theory and simulations applied to whole cell photobleach recovery. Biophys J *79*, 1761-1770.

Simons, J.F., Ferro-Novick, S., Rose, M.D., and Helenius, A. (1995). BiP/Kar2p serves as a molecular chaperone during carboxypeptidase Y folding in yeast. J Cell Biol *130*, 41-49.

Snapp, E., Altan-Bonnet, N., and Lippincott-Schwartz, J. (2003a). Measuring protein mobility by photobleaching GFP-chimeras in living cells. In: Current Protocols in Cell Biology, eds. J.S. Bonafacino, M. Dasso, J. Harford, J. Lippincott-Schwartz, and K. Yamada, New York: John Wiley&Sons, Inc., Unit 21.21.

Snapp, E.L. (2009). Fluorescent proteins: a cell biologist's user guide. Trends Cell Biol *19*, 649-655.

Snapp, E.L., Altan, N., and Lippincott-Schwartz, J. (2003b). Measuring protein mobility by photobleaching GFP chimeras in living cells. Curr Protoc Cell Biol *Chapter 21*, Unit 21 21.

Snapp, E.L., Sharma, A., Lippincott-Schwartz, J., and Hegde, R.S. (2006). Monitoring chaperone engagement of substrates in the endoplasmic reticulum of live cells. Proc Natl Acad Sci U S A *103*, 6536-6541.

Tabas, I., and Ron, D. (2011). Integrating the mechanisms of apoptosis induced by endoplasmic reticulum stress. Nat Cell Biol *13*, 184-190.

Travers, K.J., Patil, C.K., Wodicka, L., Lockhart, D.J., Weissman, J.S., and Walter, P. (2000). Functional and genomic analyses reveal an essential coordination between the unfolded protein response and ER-associated degradation. Cell *101*, 249-258.

Voeltz, G.K., Rolls, M.M., and Rapoport, T.A. (2002). Structural organization of the endoplasmic reticulum. EMBO Rep *3*, 944-950.

Welihinda, A.A., Tirasophon, W., Green, S.R., and Kaufman, R.J. (1998). Protein serine/threonine phosphatase Ptc2p negatively regulates the unfolded-protein response by dephosphorylating Ire1p kinase. Mol Cell Biol *18*, 1967-1977.

Yoshida, H., Matsui, T., Hosokawa, N., Kaufman, R.J., Nagata, K., and Mori, K. (2003). A time-dependent phase shift in the mammalian unfolded protein response. Dev Cell *4*, 265-271.

Table I: Yeast strains used in this study

Yeast strains	Description	Strain name
	BY4741 *Mat*a *ura3Δ0 leu2Δ0 his3Δ1 met15Δ0*	
Deletion array	BY4741 *ire1Δ::KanMX4*	
This work	BY4741 Kar2p-sfGFP::HIS	YPL001
This work	BY4741 *ire1Δ::KanMX4* Kar2p-sfGFP::HIS	YPL002
This work	BY4741 UPR-mCherry::URA	YPL003
This work	BY4741 Kar2-sfGFP::HIS UPR-mCherry::URA	YPL004
This work	BY4741 ER-sfGFP-HDEL::LEU	YPL005
This work	BY4741 *ire1Δ::KanMX4* ER-sfGFP-HDEL::LEU	YPL006
This work	BY4741 SR-GFP::LEU	YPL007

FIGURE LEGENDS

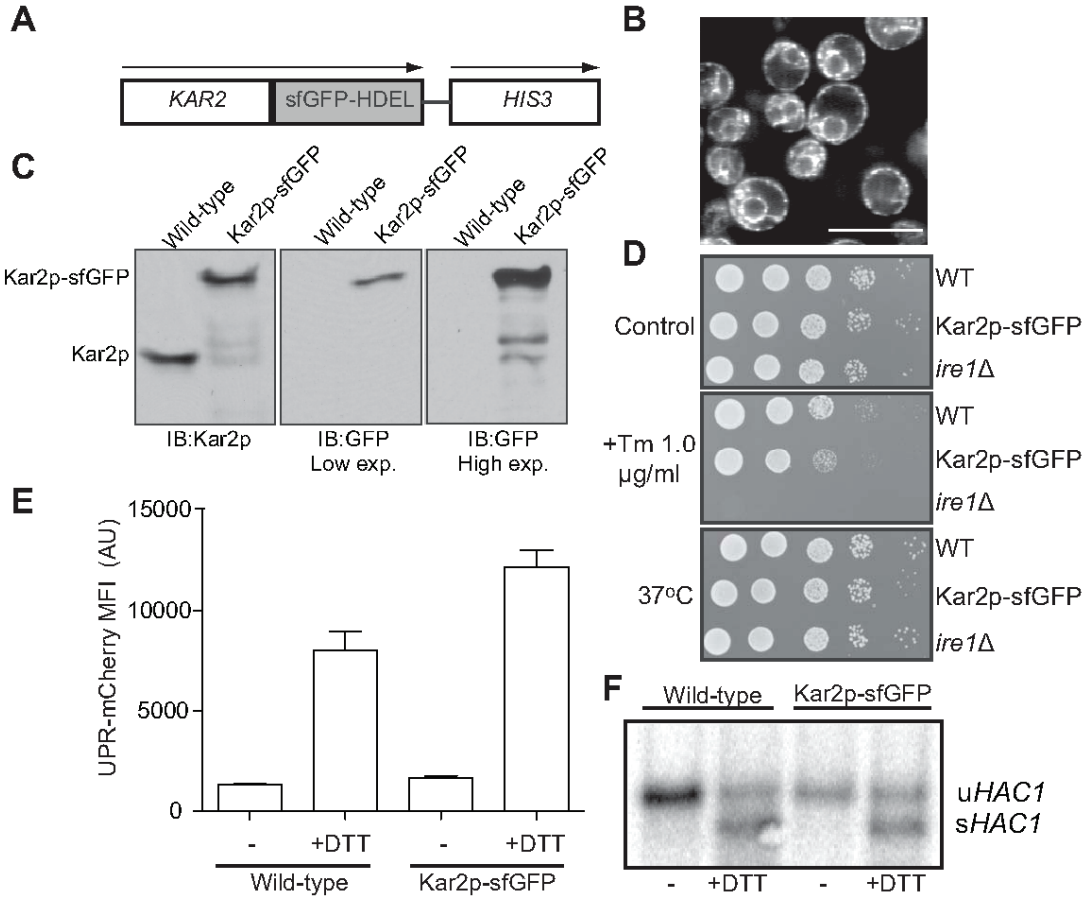

Figure 1. Expression of Kar2p-sfGFP in yeast. (A) Schematic of sfGFP-HDEL vector used to chromosomally tag Kar2p with sfGFP. Arrows indicate distinct transcription of fusion protein and selection marker. (B) Representative fluorescent image of wildtype yeast expressing Kar2p-sfGFP in a typical ER pattern. (Bar, 10 µm). (C) Immunoblots of extracts from yeast cells expressing either the endogenous Kar2p or Kar2p-sfGFP. The bands below the Kar2p-sfGFP lane in the anti-Kar2p immunoblot are also evident in a long exposure of the anti-GFP blot, indicating these are degradation products that still contain the fused sfGFP and are likely due to the high levels of proteases in yeast lysates (North, 1969). (D) Wildtype yeast strains expressing either endogenous or Kar2p-sfGFP were diluted to OD_{600nm} 0.5, serially diluted (10-fold) and spotted on plates containing 0 or 1.0 µg/ml Tm and grown at 30°C. Alternatively untreated cells were grown at 37°C to assay temperature sensitivity of the various strains. (E) Yeast cells expressing either wildtype Kar2p or Kar2p-sfGFP and the UPR-mCherry reporter were treated with 5 mM or no DTT for 1 h and analyzed by flow cytometry. Median Fluorescence Intensity (MFI) for UPR-mCherry is shown for three biological replicates. (F) RNA from yeast cells expressing either wildtype Kar2p or Kar2p-sfGFP was isolated and *HAC1* splicing was analyzed by northern blot. Unspliced (u*HAC1*) and spliced (s*HAC1*) products are indicated.

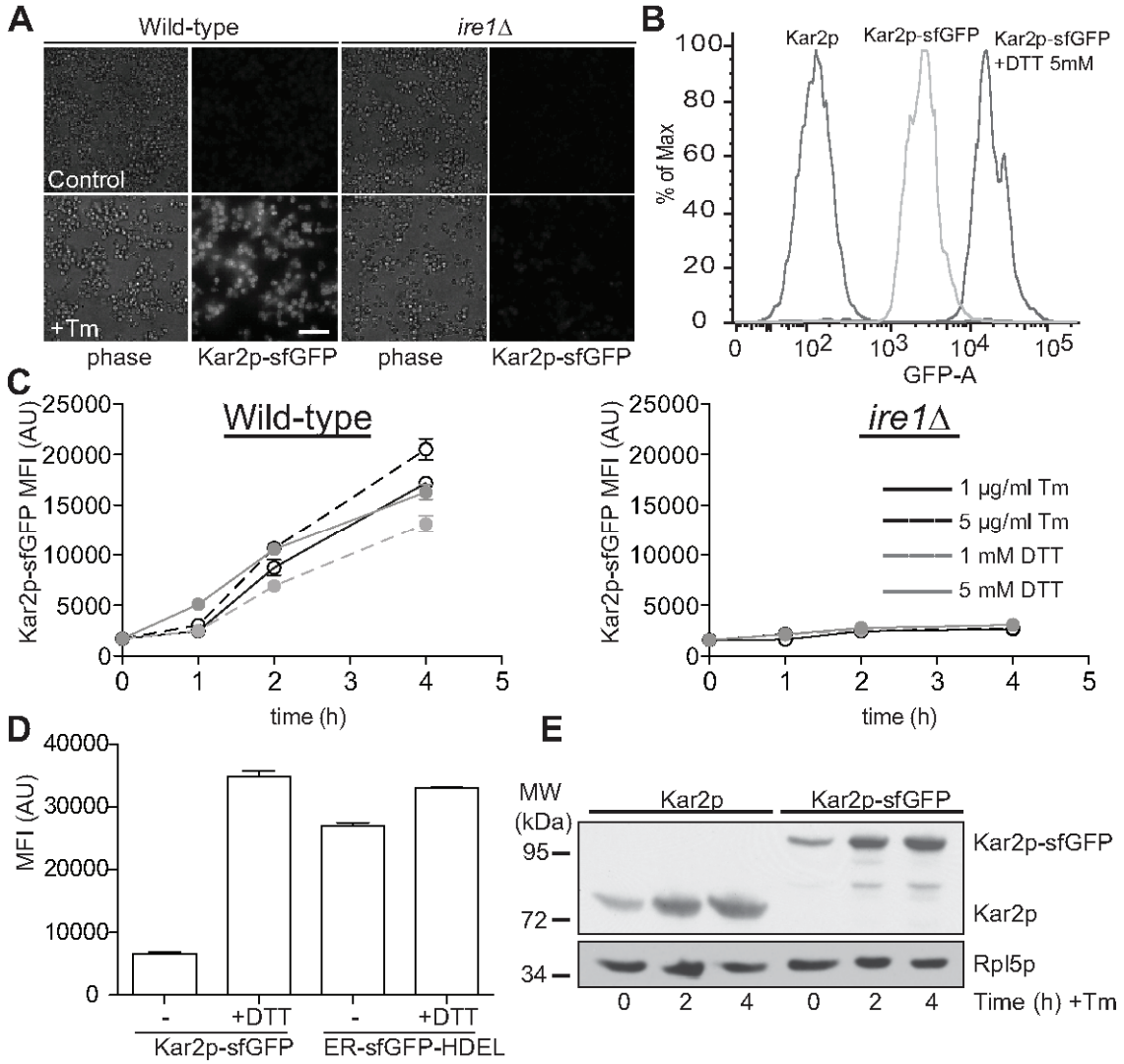

Figure 2. Increased expression of Kar2p-sfGFP following ER stress. (A) Representative phase and fluorescence images of wildtype and *ire1Δ* yeast strains expressing Kar2p-sfGFP untreated or treated with 5.0 μg/ml Tm for 4 h. (B) Yeast cells expressing wildtype Kar2p or Kar2p-sfGFP were treated with either 0 or 5 mM DTT for 4 h and analyzed by flow cytometry. Increased GFP fluorescence was detected in stressed cells. (C) Wildtype and *ire1Δ* yeast strains expressing Kar2p-sfGFP were treated with either DTT (1 or 5 mM) or Tm (1 or 5 μg/ml) and MFI values were measured at different times by flow cytometry. A functional UPR was required for stress-induced increases in Kar2p-sfGFP levels. (D) Yeast strains expressing either Kar2p-sfGFP or ER-sfGFP-HDEL were treated with 0 or 5 mM DTT for 2 h and analyzed by flow cytometry. The sfGFP MFI values are plotted. The expression of ER-sfGFP-HDEL does not change upon DTT treatment. (E) Immunoblot for Kar2p shows increased levels of both endogenous and Kar2p-sfGFP following treatment with 5 μg/ml Tm for 0, 2, and 4 h. Rpl5p served as a loading control. (Bar, 20 μm).

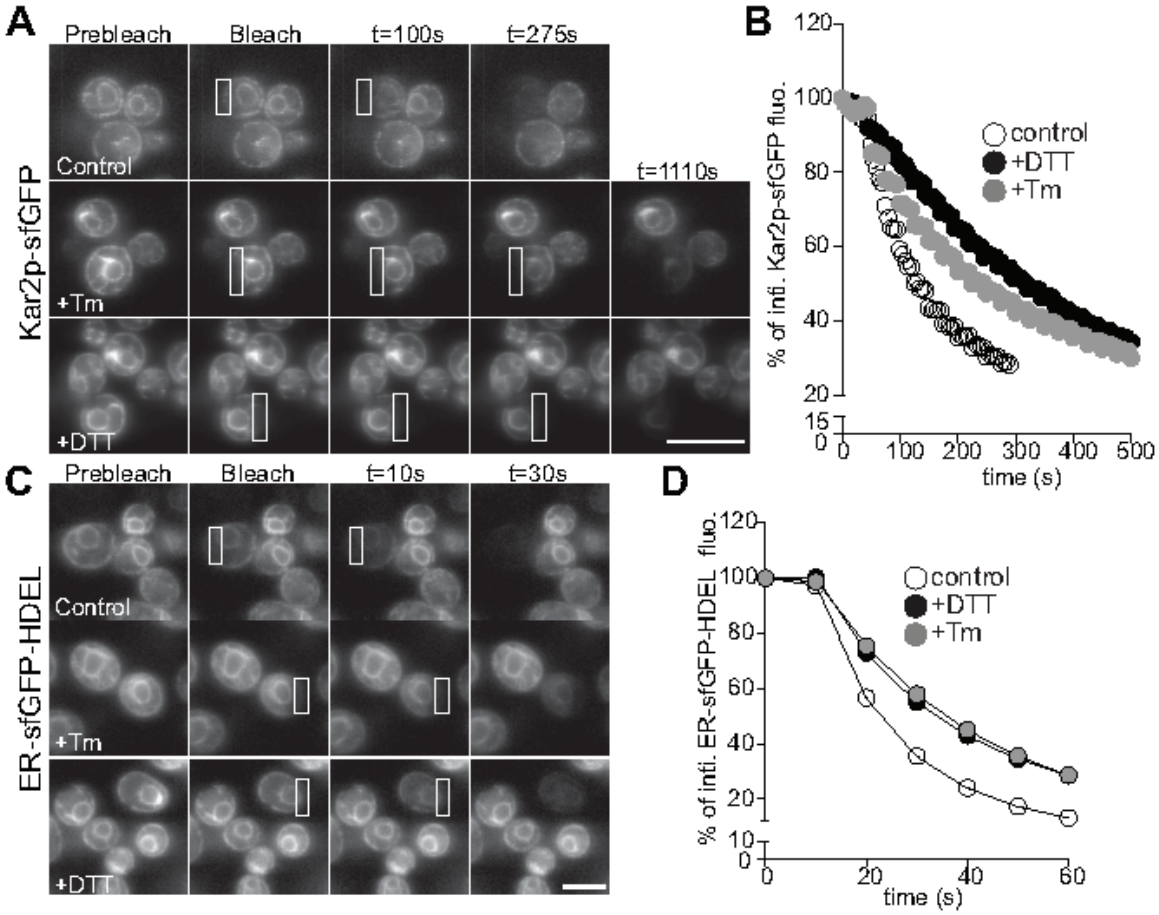

Figure 3. Kar2p is mobile under both homeostatic and stress states. FLIP series of cells repeatedly bleached in the region of interest (white box). (A) FLIP of Kar2p-sfGFP expressing yeast in early log phase untreated (top panel) or treated with either 5 mM DTT for 1 h or 1 μg/ml Tm for 2 h (lower panels). Although Kar2p-sfGFP appears to be mobile throughout the ER, stressor treated cells were depleted of fluorescence at much slower rates. (B) Plot of the mean Kar2p-sfGFP intensities during FLIP shows the faster depletion of fluorescence in untreated cells compared to DTT ant Tm treated cells (C) FLIP of ER-sfGFP-HDEL expressing yeast untreated or treated as in panel A. Depletion of cellular fluorescence is significantly faster than for Kar2p-sfGFP. (D) Plot of the mean ER-sfGFP-HDEL intensities during FLIP shows the faster depletion of fluorescence in untreated cells compared to DTT ant Tm treated cells (Bar, 10 μm).

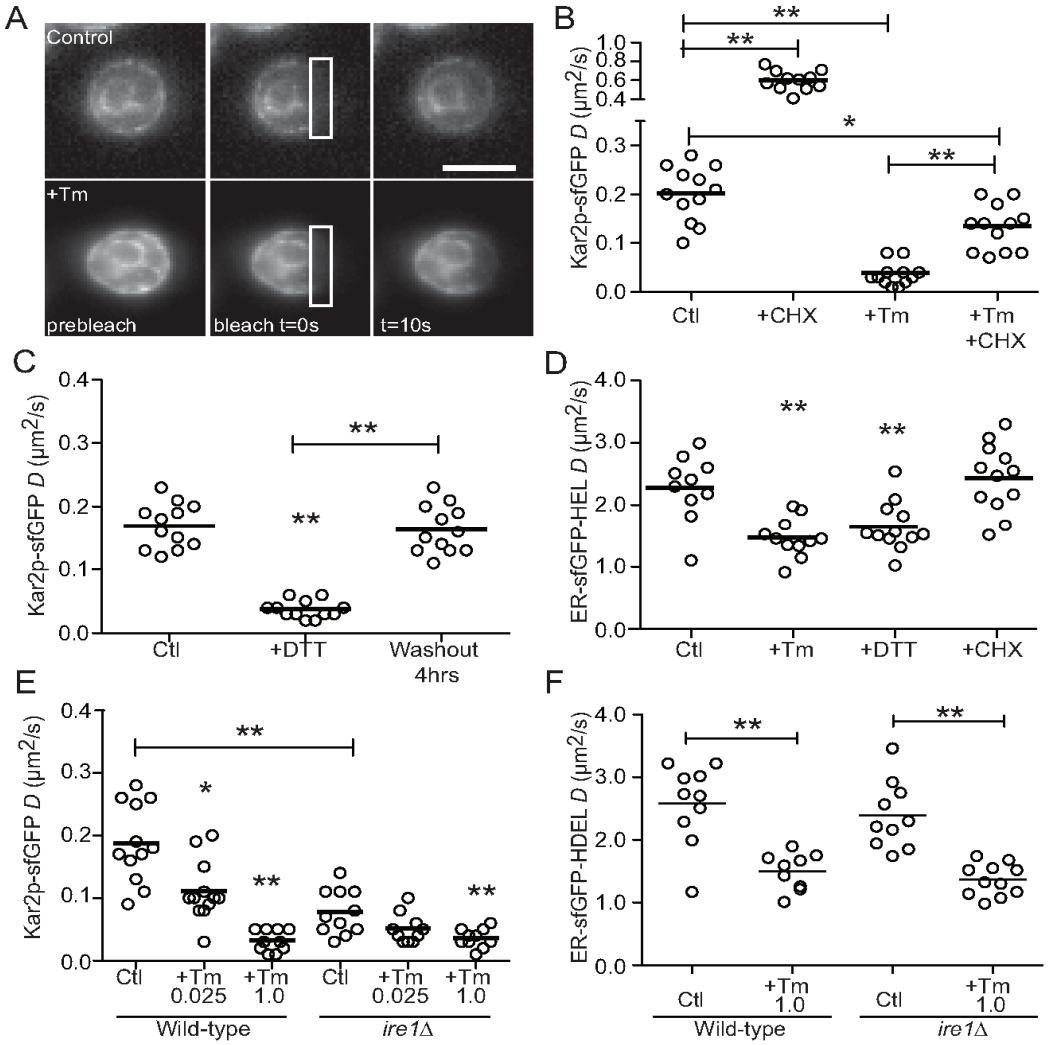

Figure 4. Kar2p-sfGFP availability quantitatively decreases during unfolded protein stress. *D* values of single cells analyzed by FRAP. (A) Representative FRAP series of cells expressing Kar2p-sfGFP. Bar: 10 μm. (B) *D* values of single Kar2p-sfGFP untreated cells, or cells treated with 10 μg/ml CHX for 30 min (+CHX), 1 μg/ml Tm for 2h (+Tm) or 1 μg/ml Tm for 2 h including 10 μg/ml CHX for the last 30 min (+Tm +CHX). (C) Reversibility of stress induced decreased Kar2p-sfGFP mobility. *D* values of single Kar2p-sfGFP untreated cells or treated with 5 mM DTT for 30 min followed by 4 h washout. (D) Small, but significant decrease in mobility of ER-sfGFP-HDEL was observed with stress suggesting an altered ER viscosity. *D* values of single ER-sfGFP-HDEL expressing cells untreated or treated with either 1.0 μg/ml Tm for 2 h, 5 mM DTT for 30 min or 10 μg/ml CHX for 30 min. (E) Kar2p-sfGFP mobility is lower in cells without a functional UPR. *D* values of single wildtype or *ire1Δ* Kar2p-sfGFP cells untreated, or treated with either 0.025 or 1.0 μg/ml Tm for 2 h are plotted. (F) Wildtype and *ire1Δ*yeast strains expressing ER-sfGFP-HDEL were treated with 1.0 μg/ml Tm for 2 h and then analyzed by FRAP. No significant changes in *D* values were observed between untreated strains. Both strains exhibited a similar significant decrease in *D* following Tm treatment. *p<0.05, **p<0.001

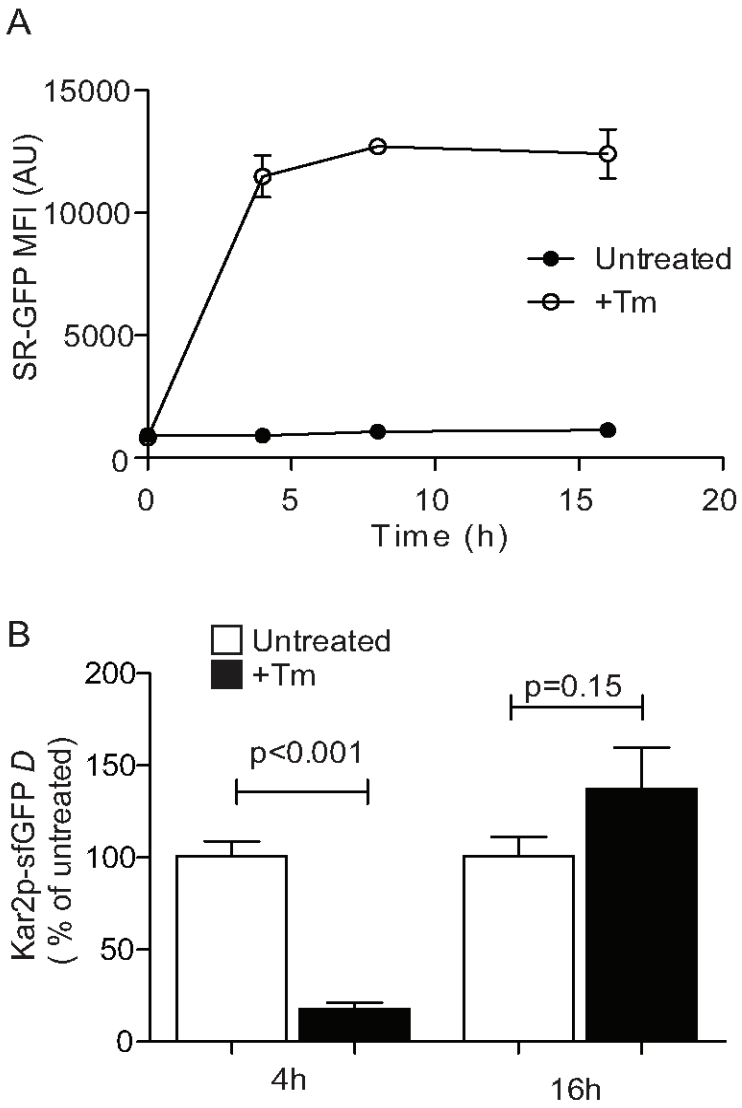

Figure 5. Kar2p availability reveals changes in the ER misfolded protein during adaptation. (A) Wild-type cells expressing the fluorescent splicing reporter (SR) consisting of GFP replacing the HAC1 ORF and produce a fluorescent signal only when spliced by ire1. SR-GFP expressing cells were treated with 1 μg/ml Tm and GFP signal was measured over time using flow cytometry. (B) Mobility of Kar2p-sfGFP untreated cells, or cells treated with 1 μg/ml Tm for 4 or 16h was measured by FRAP. Data were normalized to the mean *D* values of untreated cells for both time points. At 4h, Tm induces significant decrease in Kar2p-sfGFP mobility. Once stress is resolved and folding capacity of the ER is restored, the Kar2p-sfGFP mobility returned to the unstressed *D* values.

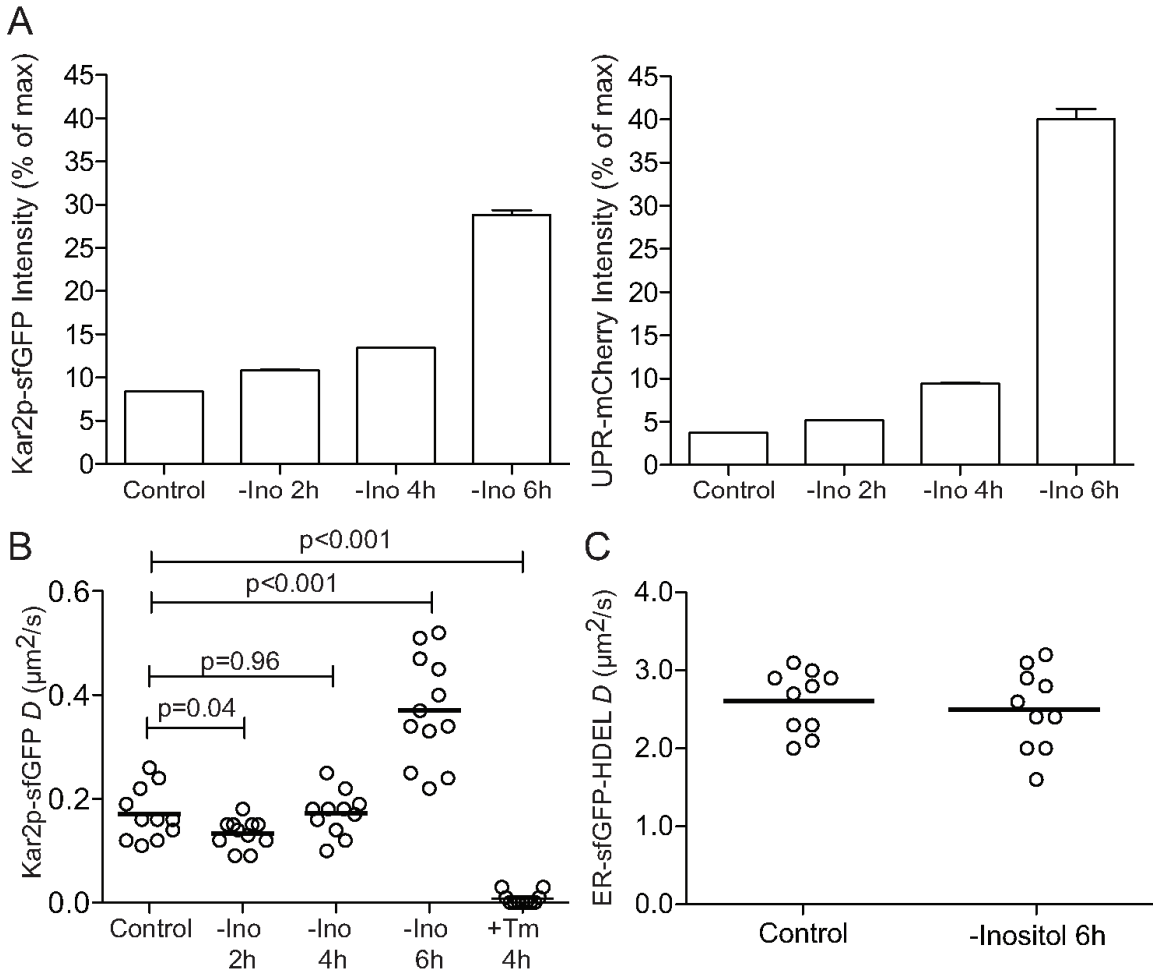

Figure 6. Kar2p availability distinguishes different forms of ER stresses. (A) Wildtype yeast expressing Kar2p-sfGFP and UPR-mCherry were incubated in inositol-minus media for indicated times and analyzed flow cytometry. MFI for the GFP (left) and mCherry (right) channels is plotted. Data are expressed as % of maximum MFI of cells treated with a robust ER stress, 1 μg/ml Tm for 4 h. (B) Time course of *D* values obtained by FRAP of single Kar2p-sfGFP cells after transfer to inositol-minus media. The reference for ER stress is 2 h treatment with 1.0 μg/ml Tm. (D) *D* values obtained by FRAP of single ER-sfGFP-HDEL expressing cells 6 h after transfer to inositol-minus media.

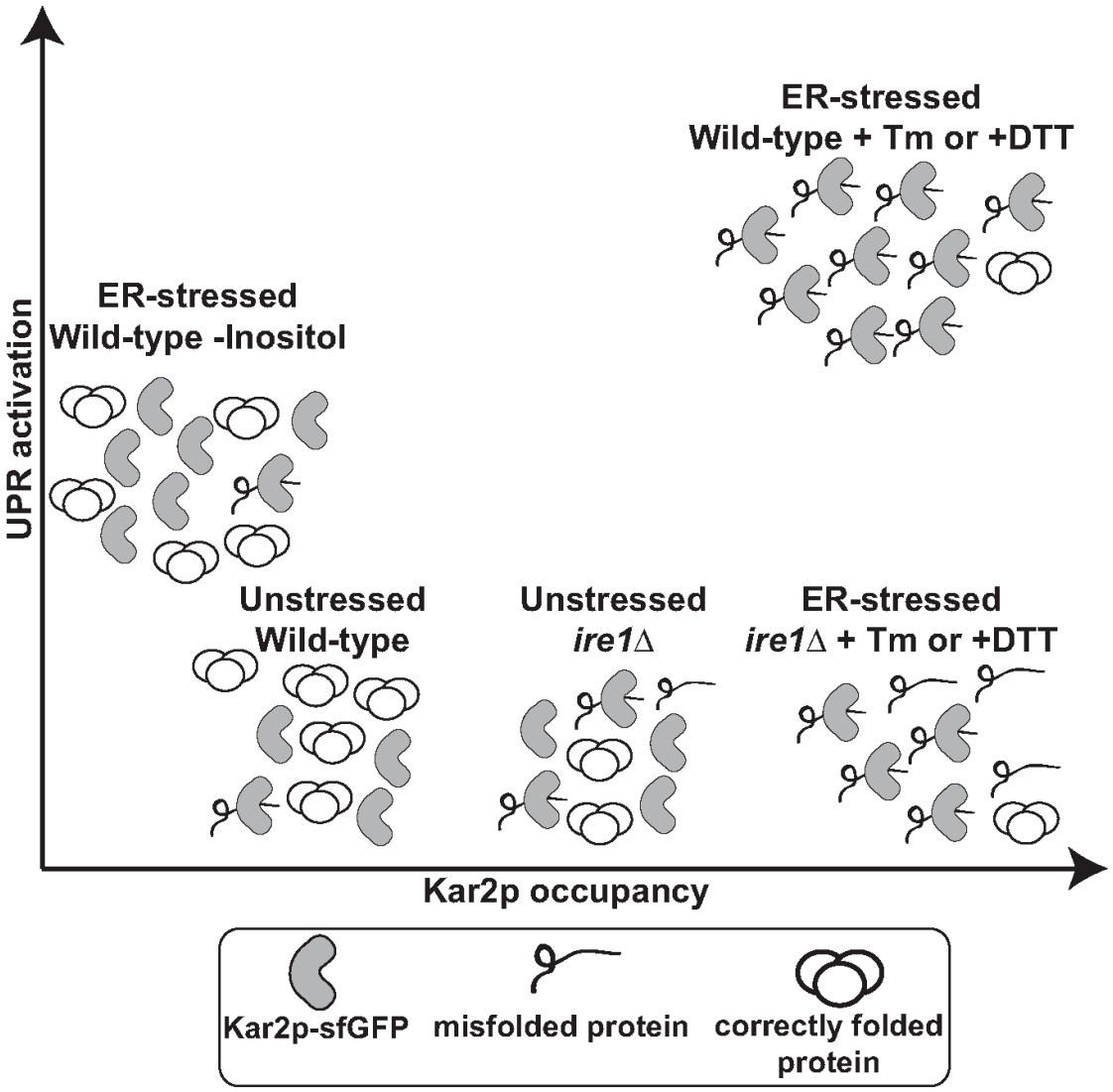

Figure 7. Conceptual model of Kar2p availability during different ER stress conditions. Decreased Kar2p availability is induced by accumulation of misfolded proteins in the ER lumen. This measurement is independent of UPR activation status and can be performed in cells lacking a functional UPR (i.e. *ire1Δ* cells). Kar2p-sfGFP occupancy defines different forms of UPR based on the ER unfolded secretory protein burden. Classical ER stressors, Tm and DTT, cause massive accumulation of unfolded protein, increase Kar2p occupancy, and lower Kar2p mobility. In contrast, depletion of inositol induces a UPR without increasing the unfolded protein burden. Kar2p mobility actually increases likely due to increased Kar2p levels without an increase in substrate levels.